Intra-day scheduling of a local energy community coordinated with day-ahead multistage decisions

(Article begins on next page)

06 February 2025

Intra-day scheduling of a local energy community coordinated with day-ahead multistage decisions

Camilo Orozco [a], Alberto Borghetti [a], Bart De Schutter [b], Fabio Napolitano [a], Giorgia Pulazza [a], Fabio Tossani [a]

[a] University of Bologna, Italy

[b] Delft University of Technology, Netherlands

***Abstract*—** The paper presents a coordinated day-ahead and intra-day approach for the scheduling of the resources in a local energy community (LEC). The considered LEC consists of a collective of power prosumers that can directly trade energy with each other in addition to the external provider. The scheduling approach is based on the alternating direction method of multipliers and aims at minimizing the total energy procurement costs, assuring that each participant has an economical advantage in being part of the community. To cope with the uncertainties of the renewable power generation and consumption during the day, a day-ahead multistage stochastic optimization approach is combined with an intra-day rolling-horizon optimization procedure. The effectiveness of the approach is supported by numerical simulations for several case studies in which the LEC prosumers are either connected to the same low-voltage network or directly to the medium-voltage level.

1. Introduction

1.1. Motivations and literature review

With the current energy transition based on renewable energy sources and distributed generation, the regulatory framework recently implemented in several countries encourages the establishment of local energy communities (LECs), where the participants agree to exploit the available resources in a coordinated way [1]. Several issues and opportunities associated with the implementation of these transactive collectives have been studied in the last years, as reviewed in e.g., [2],[3], and references therein.

One of the main aspects to be considered for the successful implementation of a LEC is the definition of an automatic energy management system (EMS) [4],[5]. Three specific aspects emerge: a) the use of distributed algorithms, b) optimization under uncertainty, and c) integrated day-ahead offline / intra-day online decision-making.

Compared to centralized ones, distributed optimization approaches have gained special interest since they ensure a reduction of the communication requirements, may be applicable to communities with a large number of participants, and help preserving the participants' privacy and independence [6]. Distributed approaches decompose the optimization procedure in several sub-problems, as shown in e.g., [4] and [7], by employing the alternating direction method of multipliers (ADMM), whilst in [8] a distributed mechanism based on game theory is proposed and in [9] both Nash equilibrium and Shapley value techniques are adopted so that the total gains and costs are distributed fairly among the participants of the LEC. Distributed

1

approaches can also exploit the implementation of blockchain or other distributed ledger technologies (see, e.g., [10],[11],[12]).

Since the forecasts of both renewable power production and energy consumption are affected by significant uncertainties, the use of stochastic optimization approaches for day-ahead scheduling is often proposed [13]–[15]. Optimization problems under uncertainty are typically addressed by a sequence of multiple stages. The day-ahead offline scheduling optimizes a probabilistic objective function: it determines a decision tree in which at each stage a set of decisions is obtained considering multiple possible future realizations. The intra-day online procedure repeatedly provides the scheduling over time considering the revealed uncertainty and updated forecasts. The integration of day-ahead and intra-day scheduling is achieved by hierarchical and online control approaches able to respond to the variations in the operational conditions (as described in e.g., [16] and references therein). In this framework, some recent papers on microgrids and multi-microgrids investigate different approaches. In [17], a hierarchical EMS adopts a multi-time scale link between the day-ahead scheduling and the intra-day operation. In [18] and [19], the day-ahead scheduling model considers the uncertainty of renewable energy generation, while a real-time dispatching model is employed to smooth out the fluctuations of generation and demand during the day. In [20] an online EMS employs a stochastic model to solve the optimal power flow of a microgrid. In [21], the day-ahead clearing decisions for an energy community are provided by an ADMM-based two-stage stochastic approach. Subsequently, a real-time deterministic model is employed by each participant in the community to perform the intra-day decisions, while keeping the day-ahead commitments. In [22], a model predictive control (MPC) technique is proposed to coordinate, in real time, the response of controllable resources of multi-networked microgrids.

Notwithstanding the several approaches documented in the literature dealing with uncertainties and real-time control issues in microgrids, this paper focuses on the development of a procedure specifically conceived for energy communities. Within this context, the typical assumption of participants' selfish behavior in the intra-day operation could affect vulnerable participants and finally the entire community. Therefore, the intra-day scheduling procedure requires considering the specific collaborative nature of a LEC, minimum human intervention, privacy requirements, and fair participation in the community providing economic advantages to all the members, also to those without generation, storage, or flexibility capabilities.

The procedure proposed in the current paper adopts the ADMM, which has the advantage to avoid auctions based on production and demand biddings with respect to mechanisms of energy market participation (as described in, e.g., [23]). Instead, by exploiting the collaborative characteristics of the community, both the scheduling of the energy resources and the prices of the transactions between LEC participants are obtained by the total efficiency optimization.

A deterministic ADMM-based approach limited to day-ahead scheduling was presented in [24]. This approach minimizes the energy procurement costs and guarantees that each participant has an economic benefit in being part of the community with respect to the case in which the prosumers can exchange only with the external energy provider (assumed to be the utility for the sake of simplicity). In [25], a day-ahead multistage stochastic scheme is adapted to the ADMM scheduling model of a LEC. The day-ahead solution is used to implement recurrent decisions during the day. An intra-day selection procedure is implemented that, at the end of each stage, finds the best fit between the revealed net power profiles for each prosumer and the scenarios considered in the day-ahead procedure. In [25], the solution during the day is updated according to the conditions at the end of each stage. Nevertheless, the set values associated with the possible solutions at each stage are limited to day-ahead calculations.

1.2. Contributions and paper organization

This paper combines and extends the work presented in previous papers [24] and [25] focusing on the development of a rolling-horizon distributed optimization procedure for the intra-day scheduling that is coordinated with the decision tree provided by a multistage stochastic day-ahead scheduling. With respect to the deterministic approach presented in [24], the current paper considers the uncertainties associated with the forecasts of local generation and energy demand in the community during the day. For this purpose, the paper presents a multistage stochastic programming approach for the day-ahead scheduling, coupled with a rolling-horizon intraday procedure not considered in [25].

In proposed scheme, a decision tree defines consecutive actions during the day in response to the possible realizations of photovoltaic (PV) generation and energy consumption at each stage (i.e., consecutive time steps grouped according to common decisions). The implementation of such a multistage scheme allows the intra-day procedure to select the operational schedule of the LEC during the day by using updated information, in contrast to a day-ahead solution based on forecast profiles, in which a single scheduling is determined for the entire day. The intra-day optimization procedure can mitigate the effect of the fluctuations in energy generation and demand, although it is solved within the fixed time limits and keeps the advantages provided by the distributed structure.

This framework is suitable for the implementation in the automatic EMS of a community.

The main contributions can be summarized as follows:

- an ADMM-based procedure is employed in all phases of the optimization, preserving the collaboration objectives and privacy requirements of LEC participants, with the guarantee that all LEC participants can reduce their costs or increase their revenues;
- the day-ahead multistage stochastic optimization provides a decision tree for the next day, allowing to divide the optimization horizon into several stages in which the best choices can be selected by using

updated information without compromising the overall daily cost minimization;

- at each time step t, the intra-day rolling-horizon optimization provides the coordinated scheduling of battery energy storage (BES) units and energy transactions inside the LEC based on the uncertainty realization and updated predictions for energy generation and load demand.

The approach can deal with prosumers equipped with different types of generating/storage units and with consumers able to offer some level of demand flexibility. Three different case studies of communities with several PV units and BES systems are considered for testing. For each case study, the effectiveness of the proposed intra-day approach has been studied by testing its performance under several operational conditions. Additionally, the numerical tests included an analysis of the individual performance of each participant in the LEC.

The structure of the paper is as follows. Section 2 presents the proposed approach. Section 3 focuses on the offline day-ahead multistage stochastic optimization of the LEC. Section 4 focuses on the online intra-day scheduling of the energy resources in the LEC. Section 5 presents the test results. Finally, Section 6 concludes the paper.

2. Scheme of the proposed approach

The considered LEC corresponds to a set of several prosumers denoted as $\Omega = \{1, 2, \ldots, N\}$. The participants in the LEC are equipped with PV units, BES units, and loads. Set $T = \{1, 2, \ldots, t_{\text{end}}\}$ denotes the set of time steps t in the optimization horizon.

As in the deterministic day-ahead scheduling approach presented in [24], the objective function (OF) to be minimized is the daily energy procurement cost. In the centralized model, OF is the cost associated with the power exchanges $P^t_{\text{buy\_Grid}\,i}$ and $P^t_{\text{sell\_Grid}\,i}$ of each prosumer with the utility during the day, taking into account the corresponding prices of buying and selling (π^t_{buy} and π^t_{sell}, respectively). Thus, the centralized OF is given by

$$OF = \sum_{\substack{t \in T \\ i \in \Omega}} \left(\pi^t_{\text{buy}} P^t_{\text{buy\_Grid}\,i} - \pi^t_{\text{sell}} P^t_{\text{sell\_Grid}\,i} \right) \Delta t \tag{1}$$

where prices π^t_{buy} and π^t_{sell} are assumed to be known. The time step size is denoted as Δt.

In the distributed optimization, based on the ADMM algorithm carried out iteratively in a sequential manner [26], the OF is decomposed in local subproblems, one for each prosumer i:

$$OF_i = \operatorname*{minimize}_{\substack{P_{\text{buy\_Grid }i}^t,\, P_{\text{sell\_Grid }i}^t \\ P_{\text{buy }i,j}^t,\, P_{\text{sell }i,j}^t}} \sum_{t\in T}\left[\begin{array}{c} \pi_{\text{buy}}^t P_{\text{buy\_Grid }i}^t \Delta t - \pi_{\text{sell}}^t P_{\text{sell\_Grid }i}^t \Delta t + \\ \displaystyle\sum_{\substack{j\in\Omega \\ j\neq i}} \lambda_j^t P_{\text{buy }i,j}^t \Delta t - \lambda_i^t \sum_{\substack{j\in\Omega \\ j\neq i}} P_{\text{sell }i,j}^t \Delta t + \ell_i^t \end{array}\right] \tag{2}$$

where profiles $P_{\text{buy }i,j}^t$ and $P_{\text{sell }i,j}^t$ represent the power bought/sold by prosumer i from/to prosumer j at each time step t, respectively. Lagrangian multipliers λ_i^t and λ_j^t are associated to the equilibrium between energy sold and bought in each internal transaction. Term ℓ_i^t penalizes the imbalances in the energy exchanges between i and every other prosumer by using parameter ρ and scale factor m:

$$\ell_i^t = m\cdot\rho\cdot\left[\sum_{\substack{j\in\Omega \\ j\neq i}} (\hat{P}_{\text{buy }j,i}^t - P_{\text{sell }i,j}^t)^2 + \sum_{\substack{j\in\Omega \\ j\neq i}} (P_{\text{buy }i,j}^t - \hat{P}_{\text{sell }j,i}^t)^2\right] \tag{3}$$

where the $\hat{P}_{\text{buy }j,i}^t$ and $\hat{P}_{\text{sell }j,i}^t$ denote the resulting profiles of the local optimization of prosumer j. As the ADMM is solved in series, these values are the most updated available at the current iteration. The ADMM iteratively adjusts the Lagrangian multipliers until the imbalances of (3) are lower than a predefined tolerance ε.

For a detailed review of the prosumer model and convergence considerations of the ADMM algorithm the reader is referred to [24]. The model of each prosumer includes the following power balance constraint

$$\begin{aligned} P_{\text{PV }i}^t + P_{\text{dis }i}^t + P_{\text{buy\_Grid }i}^t + \sum_{\substack{j\in\Omega \\ j\neq i}} P_{\text{buy }i,j}^t &= P_{\text{Load }i}^t + P_{\text{ch }i}^t \\ + P_{\text{sell\_Grid }i}^t + \sum_{\substack{j\in\Omega \\ j\neq i}} P_{\text{sell }i,j}^t &+ \frac{1}{2}\sum_{b\in B} L_{b,i}^t \qquad t\in T, i\in\Omega \end{aligned} \tag{4}$$

Constraint (4) takes into account the PV production ($P_{\text{PV }i}^t$), the local load ($P_{\text{Load }i}^t$), the battery charging and discharging power ($P_{\text{ch }i}^t$ and $P_{\text{dis }i}^t$, respectively), the transactions with other participants ($P_{\text{sell }i,j}^t$ and $P_{\text{buy }i,j}^t$), the power exchange with the external grid ($P_{\text{buy\_Grid }i}^t$ and $P_{\text{sell\_Grid }i}^t$) at each time step t and the estimation of the losses $L_{b,i}^t$ in branch b due to transactions involving prosumer i. Since each transaction is between two prosumers, only half of the power loss is attributed to each prosumer. The corresponding loss estimates and their allocation to each prosumer are obtained by the piece-wise linearization of the quadratic relationship between the Joule losses in a branch and the power flows caused by all the transactions involving the considered prosumer (constraints (12)-(16) in [24]). For each prosumer, simultaneous buying and selling processes at each time step t are avoided by indicator constraint (5) and binary variable u_i^t:

$$\begin{cases} P_{\text{buy\_Grid }i}^t = 0 \text{ and } P_{\text{buy }i,j}^t = 0 \text{ if } u_i^t = 0 & u_i^t \in \{1,0\} \\ P_{\text{sell\_Grid }i}^t = 0 \text{ and } P_{\text{sell }i,j}^t = 0 \text{ if } u_i^t = 1 & i,j\in\Omega \end{cases} \tag{5}$$

Furthermore, the stored energy in the BES unit i, denoted as $E_{\mathrm{BES}\,i}^{t}$, is defined at each time step t considering charging and discharging efficiencies ($\eta_{\mathrm{ch}\,i}$ and $\eta_{\mathrm{dis}\,i}$, respectively) by using the following constraints:

$$E_{\mathrm{BES}\,i}^{t} = E_{\mathrm{BES}\,i}^{t-1} + (P_{\mathrm{ch}\,i}^{t}\eta_{\mathrm{ch}\,i} - P_{\mathrm{dis}\,i}^{t}/\eta_{\mathrm{dis}\,i})\Delta t \quad \begin{array}{c} i \in \Omega \\ t \in T, t > 1 \end{array} \tag{6}$$

$$\begin{cases} E_{\mathrm{BES}\,i}^{t=1} = E_{\mathrm{max},i} + (P_{\mathrm{ch}\,i}^{t=1}\eta_{\mathrm{ch}\,i} - P_{\mathrm{dis}\,i}^{t=1}/\eta_{\mathrm{dis}\,i})\Delta t \quad i \in \Omega \\ E_{\mathrm{BES}\,i}^{t_{\mathrm{end}}} = E_{\mathrm{BES}\,i}^{\max} \quad i \in \Omega \end{cases} \tag{7}$$

$$0 \le P_{\mathrm{dis}\,i}^{t} \le P_{\mathrm{BES}\,i}^{\max} \quad 0 \le P_{\mathrm{ch}\,i}^{t} \le P_{\mathrm{BES}\,i}^{\max} \quad t \in T, i \in \Omega \tag{8}$$

$$E_{\mathrm{BES}\,i}^{\min} \le E_{\mathrm{BES}\,i}^{t} \le E_{\mathrm{BES}\,i}^{\max} \quad t \in T, i \in \Omega \tag{9}$$

In constraint (8), the maximum value $P_{\mathrm{BES}\,i}^{\max}$ limits the discharge and charge power. Constraint (9) limits the stored energy between a minimum level $E_{\mathrm{BES}\,i}^{\min}$ and a maximum level $E_{\mathrm{BES}\,i}^{\max}$.

In the present paper, the LEC scheduling is defined though the coordination of the day-ahead and intra-day phases, as illustrated in Fig. 1.
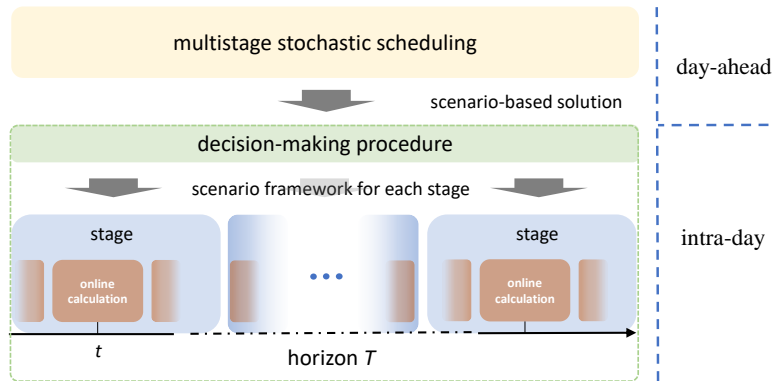
Fig. 1 Scheme of the coordinated day-ahead and intra-day strategy for the LEC scheduling.

First, the day-ahead operational plan is modelled as a multistage stochastic optimization problem, in which the horizon time (a day) is divided into various stages, i.e., consecutive time steps grouped according to common decisions. In this phase, the response to the uncertainties associated with the local generation and loads are represented by a tree of decisions. The corresponding multistage solution, which is obtained by using the ADMM procedure, provides a set of decisions for the operation of the BES units and energy transactions inside the LEC at each stage.

Then, during the intra-day phase, the solutions of the day-ahead multistage model are used as an operational framework for the online decision-making procedure, which is carried out by the LEC during the day. Within this framework, the decisions made at each time step t are defined by an online calculation that involves a distributed rolling-horizon optimization (see, e.g. [27]). The coordinated approach allows the LEC

to adjust accurately its set values according to the current operational conditions at each time step t (based on measurements of PV generation and load).

The use of a multistage scheme allows the adoption of corrective decisions at some predefined instants during the day to cope with fluctuations in photovoltaic production and load consumption. Indeed, the multistage stochastic solution provides a set of feasible alternatives at the end of each stage that allow to adapt the scheduling of the decision variables based on previous observations The exploitation of this possibility is expected to provide more efficient results with respect to approaches in which a single 24-hour scheduling decision is made at the beginning of the day.

In the implemented approach, the 4-stage day ahead model provides a decision tree with an initial scheduling and a set of alternative solutions at 8 am and 4 pm. The intra-day procedure then selects the best alternative path in the tree based on the realization of the stochastic processes (photovoltaic production and load consumption) and the available updated forecasts.

In the following sections, the implementation of the scheduling approach during the day-ahead and intra-day phases, and their coordination are described.

3. Day-ahead multistage stochastic scheduling

In order to deal with the uncertainties associated with the distributed generation and loads consumption, the day-ahead distributed model of [24] has been extended to a multistage stochastic approach.

In the multistage model, an adequate representation of the stochastic variables is required. This representation defines when the decisions are to be made and when the observations are to be revealed, while employing a finite number of scenarios to maintain the tractability of the problem. The realization of the stochastic processes in the LEC, during the day, is represented by a scenario tree.

For the numerical tests included in this paper the day-ahead time horizon has been divided into three decision stages, where the decisions are made at the beginning of each stage (i.e., every eight hours). Variables $P_{\text{ch } i}^t$ and $P_{\text{dis } i}^t$ are assumed as the decision variables of the model. The other variables are calculated at the end of each stage, for all time step t in stage s.

In the following, first the procedure adopted for the construction of the scenario tree is described. Then, the scenario tree is used by the day-ahead multistage scheduling presented in this section to obtain the corresponding decision tree. The online intra-day scheduling is coordinated with the decision tree as described in Section 4.

3.1. Scenario-tree model

We adopt for each prosumer a scenario generation technique that applies a Markov-process considering the autocorrelation between consecutive observations starting with the forecast profiles of PV production and

load, as described in [28]. The scenario generation procedure limits the deviation of the stochastic variables $P_{\text{Load}\,i}^t$ and $P_{\text{PV}\,i}^t$ to the $\pm 20\%$ of the given forecast profile at a given time step t, for the 100% and 75% of the time, respectively. The definition of these tolerance bands avoids unrealistic scenarios and guarantees that the generated scenarios are coherent with the forecast profiles.

Let us define a set of equiprobable scenarios for each prosumer i denoted with Φ_i. Index φ_i denotes the scenario index corresponding to i. From Φ_i, a scenario profile $\xi_{\varphi_i}^t$ is denoted as the difference between PV production and load in scenario φ_i, normalized by the difference of the relevant forecast profiles of i at each time step t, namely

$$\xi_{\varphi_i}^t = \frac{P_{\text{PV}\,\varphi_i}^t - P_{\text{Load}\,\varphi_i}^t}{P_{\text{PV}\,i}^t - P_{\text{Load}\,i}^t} \tag{10}$$

The prosumers share the obtained values of $\xi_{\varphi_i}^t$ with the community. In this way, the participant in the LEC does not reveal private information, since neither the forecast values of PV generation nor demand are shared. Then, a set Γ of scenarios is obtained. Each one of these equiprobable $N \times T$-dimensional scenarios (with N equal to the number of prosumers and T the number of time steps) is defined by the structure

$$\psi_\varphi = \left[\xi_{\varphi_1}^t, \xi_{\varphi_2}^t, \ldots, \xi_{\varphi_N}^t \right] \tag{11}$$

Next, a tree is obtained by a *k*-means clustering procedure applied to the total set of initial scenarios, with the scenario reduction technique described in [28]. The relevant probability of each scenario in the tree at each stage corresponds to the summation of the probabilities of each ψ_φ classified in the corresponding cluster.

The structure of the obtained tree is influenced by the number of initial scenarios. Therefore, a large number is used without compromising the tractability of the clustering procedure.

The clustering procedure may be carried out by a coordinator unit and then communicated to the participants or by each one of the prosumers, obtaining the same common scenario tree for all the participants and preserving the distributed scheme.

The choice of the number of clusters K is influenced by the data structure (i.e., complexity and structure of the samples) and the search for acceptable solution time and computational effort. Typically, for this purpose, the so-called elbow method and the silhouette coefficient are adopted. As described in, e.g., [29], the elbow method looks for a reduction in the average distance of the aggregated data to the relevant centroid (i.e., the average value of sum of the squared errors *SSE* calculated for each scenario).

The silhouette coefficient for each scenario ψ_φ is given by

$$s(\psi_\varphi) = \frac{b(\psi_\varphi) - a(\psi_\varphi)}{\max\left(a(\psi_\varphi), b(\psi_\varphi)\right)} \tag{12}$$

where $a(\psi_\varphi)$ is the mean intra-cluster distance (i.e., distance of a sample to the other samples in the cluster) and $b(\psi_\varphi)$ the mean nearest-cluster distance (i.e., distance of a sample to all the samples in the nearest-cluster) of each scenario. The average value of $s(\psi_\varphi)$ shows how well the scenarios have been classified.

In contrast with the elbow method, which is based entirely on intra-cluster calculations, the silhouette coefficient also considers the separation with respect to the neighboring clusters, allowing to better avoid misclassified samples. A high coefficient value is desired to reduce the intra-cluster dissimilarities (i.e., good cohesion) and to increase the inter-cluster dissimilarities (i.e., avoiding the presence of outliers).

For illustrative purposes, Table 1 shows the values obtained for the average *SSE* and the average of the silhouette coefficient for the first eight hours of the day and for several number of clusters in case study A, described in Section 5.

Although the average *SSE* decreases with the number of clusters, the highest average value of the silhouette coefficient is obtained by three clusters indicating that the accuracy of the aggregation could be undermined by a high number of centroids. This justifies the adoption of three centroids for the numerical tests presented in this paper.

Table 1
Elbow method and silhouette coefficient metrics for the selection of the number of clusters: Case A.

Number of clusters	3	4	5	6	7	8	9
Average SSE	98.9	79.1	72.1	63.9	52.5	47.1	40.4
Average $s(\psi_\varphi)$	0.54	0.53	0.52	0.50	0.53	0.50	0.51

The multistage stochastic optimization of the day-ahead scheduling decision model is based on the construction of the scenario tree [30].

Fig. 2 shows the tree obtained for the LEC in case study A, as well as the probability associated with each scenario ψ_φ. The scenarios indicated in parenthesis in Fig. 2 are the centroids obtained by the clustering procedure. At stage 1 (beginning of the day) the actual state of the system is assumed to be known; therefore, the tree has a single root; so a single decision should be made for the first 8 hours. Such a decision is based on a single centroid evaluated for the entire set of scenarios, which is scenario 196 for the considered test case. The possible realization of the stochastic variables in the first 8 hours is represented by three centroids, namely Scen-174, Scen-196, and Scen-197. The three states at stage 2, one for each centroid, represent the states of the community at 8 am when the second stage decision should be made. Analogously, for each of the 3 states at 8 am, namely (Scen-174,2), (Scen-196,2), and (Scen-197,2), the stochastic model between

9

8 am and 4 pm is described by three centroids. For each of the states at 4 pm, other three centroids represent the stochastic model between 4 pm and midnight.

The decisions of the multistage optimization described in the next Section 3.2 are made at the beginning of the day, time step 33 (8 am), and time step 64 (4 pm). These decisions are anticipative variables. In the considered test case, these variables are the scheduling of the batteries (i.e., $P_{\mathrm{ch}\,i}^t$ and $P_{\mathrm{dis}\,i}^t$) for the 32 time steps following the decision. At each of the $3 \times 32 = 96$ time steps, other variables are also calculated (such as the power flows, energy exchanges, costs, and revenues). These adaptive variables depend on previous decisions and the observed outcomes of the stochastic events. Since the total daily cost and revenues (i.e., the value of the objective function) are obtained at time step 96 (midnight), Fig. 2 indicates 4 stages: the three that correspond to the instants when the anticipative decisions are made and, as fourth stage, the instant when the value of the objective function is obtained.
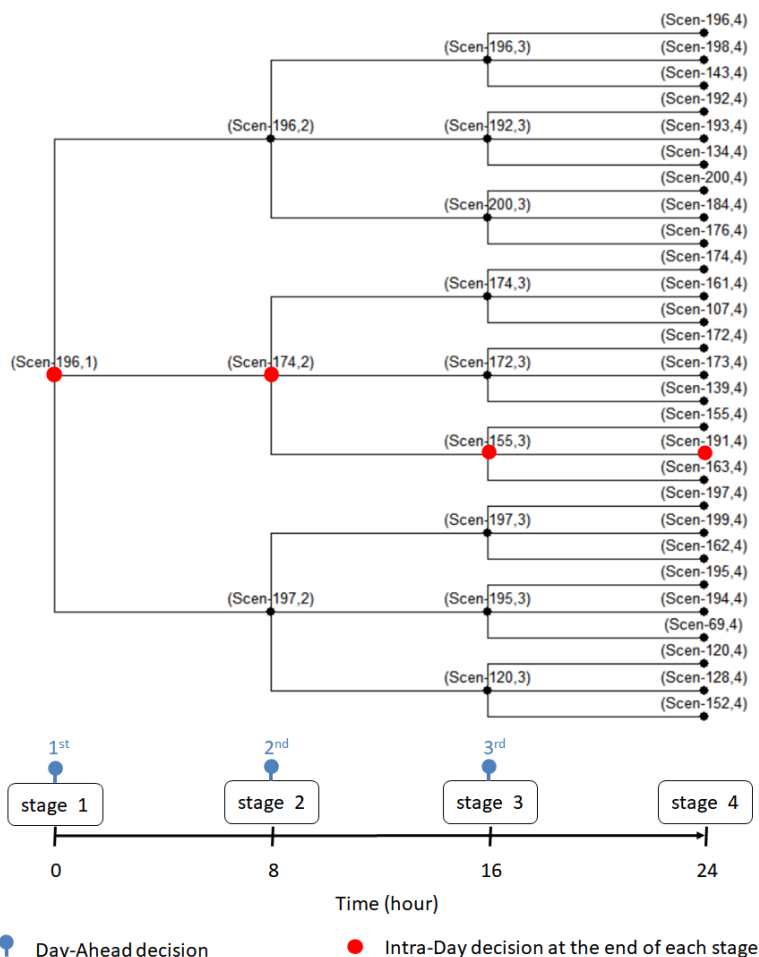

Fig. 2. Tree of the aggregated scenarios using three clusters for case study A and of the decisions. In blue, set of day-ahead decisions. In red, an example of the decisions selected by the intra-day decision-making procedure at the end of each stage.

10

3.2. Multistage stochastic solution

The stochastic version of the LEC scheduling problem is given by

$$\sum_{\varphi} \pi_{\varphi} \left(\sum_{i} OF_{i}^{\varphi} \right) \tag{13}$$

where π_{φ} is the probability associated with each scenario ψ_{φ} included in the scenario tree. The solution for each one of these scenarios is found by means of the ADMM procedure, where the values of $P_{\text{PV}\,i}^{t}$ and $P_{\text{Load}\,i}^{t}$ are given by the corresponding scenario ψ_{φ}, and the resulting daily costs for each prosumer i are represented by OF_{i}^{φ}.

This solution provides the optimal set values of the decision and wait-and -see variables at each node of the tree. Non-anticipativity constraints (see, e.g., [31]) bind the decision variables to be equal at every common node for those scenarios that partially share the same path from the root to the leaf.

In view of the above, each node of the tree in Fig. 2, at stages 2 and 3, represents an alternative decision obtained by the solution of the multistage stochastic problem. The collection of all the decision variables values at each stage 1, 2, and 3 constitutes the decision tree for case study A.

The intra-day solution procedure choses the most appropriate decision by considering, at stage 2, the observed outcomes before 8 am and, at stage 3, those observed before 16 h, as described in the next section. In Fig. 2, the red dots represent an example of the decisions provided by the intra-day decision-making procedure. For the first eight hours of the day, the LEC considers the operational scenario denoted as Scen-196. Then, the red dot at (Scen-174,2) represents the decision selected by the intra-day solution for stage 2 if the actual realization of the stochastic variables in the first 8 hours is like scenario 174. Afterward, the red dot in (Scen-155,3) indicates the decision selected by the intraday procedure for stage 3 if the actual realization of the stochastic variables in the interval 8h – 16 h is close to scenario 155. The red dot at (Scen-191,4) indicates that the closest scenario in the day-ahead tree to the actual realization of the stochastic variables between 16 h and 24 h is scenario 191. The objective function value in node (Scen-191,4) indicates the daily cost and revenues of the community in the considered example.

4. Intra-day scheduling of the LEC based on rolling-horizon online optimization

The implementation of the multistage solution based on decisions at the end of each stage allows the LEC to respond in a flexible way to the fluctuations of the PV generation and the load throughout the day. However, for practical considerations, the number of stages should be limited. To define an improved intra-day solution also in cases of significant deviations from the day ahead forecasts, the intra-day decision-making procedure coordinates the multistage day-ahead solution with an online calculation that adjusts the

operational set values also during the stages, at every time-step t. The subset of T that contains the successive time steps t in stage s is denoted as T^s.

By means of the Euclidean distance, the intra-day decision-making procedure identifies the scenario of the tree that best matches the profile of the difference between the local generation and the energy demand up to time step t. Each prosumer performs its own comparison of the local profiles and shares the corresponding distance with the others to make a joint decision based on the structure of the common tree.

The operational scenario for each stage is defined by the expected profiles of $P_{\text{PV } i}^t$ and $P_{\text{Load } i}^t$ for all the time steps during the stage, and the corresponding decision-variables values of the BES units. Then, the online optimization is carried out for the current step t_m, based on the available measurement of PV generation and load as illustrated in Fig. 3.
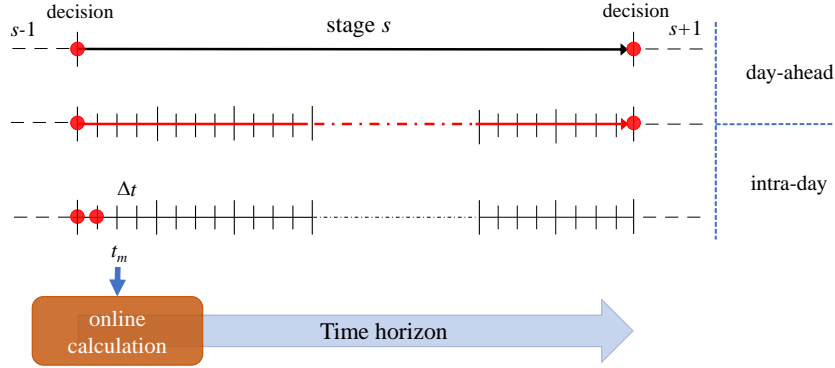

Fig. 3. Scheme for the coordinated scheduling of the LEC at each stage.

Like a rolling-horizon control or MPC strategy, the online optimization considers the horizon from the current time step t_m until the last time step in T^s and it is carried out by each prosumer. Only the operational set values calculated for t_m are implemented. The calculation and the implementation of the solutions is repeated for the following time steps up to the end of the stage. As already mentioned, the online optimization employs an ADMM distributed procedure, with the following characteristics:

- *Implementation of a parallel scheme*

A short calculation time in comparison with the duration of each Δt is obtained by a parallel scheme of the consensus ADMM algorithm. For the online calculation, expression (3) is replaced by

$$\ell_i^t = m \cdot \rho \cdot [\sum_{\substack{j \in \Omega \\ j \neq i}} (\overline{P}_{\text{exc } j,i}^t - P_{\text{sell } i,j}^t)^2 + \sum_{\substack{j \in \Omega \\ j \neq i}} (P_{\text{buy } i,j}^t - \overline{P}_{\text{exc } i,j}^t)^2] \tag{14}$$

where

$$\overline{P}_{\text{exc } i,j}^t = \frac{1}{2}(\hat{P}_{\text{buy } i,j}^t + \hat{P}_{\text{sell } j,i}^t) \tag{15}$$

in this case, parameters $\hat{P}^t_{\text{buy } i,j}$ and $\hat{P}^t_{\text{sell } j,i}$ are equal to the corresponding profiles obtained at the previous iteration.

- *Stored energy in the BES units at the end of each stage as an operational condition*

The stored energy in the BES units at the end of the stage are fixed according to the result of the decision-making procedure. At the end of each stage (e.g., 8 am and 4 pm), the intra-day decision-making procedure provides the scenario of the tree that better fits the expected PV and load conditions during the next stage (i.e., 8 hours). The day-ahead multistage stochastic solution that corresponds to the selected scenario provides the stored energy at the end of the next stage. In this manner, the set values of the day-ahead optimization are exploited as an operational condition for the batteries during each stage. This reduces the number of variables (i.e., the associated computational effort), while keeping the good quality of the results. For such a purpose, in the intra-day implementation, the initial and final energy in the BES unit during the stage are constrained by

$$
\begin{cases}
E^{t=t_1^s}_{\text{BES } i} = E^{\text{initial}^s}_{\text{BES } i} + (P^{t=t_1^s}_{\text{ch } i}\, \eta_{\text{ch } i} - P^{t=t_1^s}_{\text{dis } i}\, /\, \eta_{\text{dis } i})\Delta t \\
E^{t=t^s_{\text{end}}}_{\text{BES } i} = E^{\text{final}^s}_{\text{BES } i}
\end{cases}
\tag{16}
$$

where t_1^s corresponds to the first time step of stage s; t^s_{end} represents the last time step of stage s; $E^{\text{initial}^s}_{\text{BES } i}$ and $E^{\text{final}^s}_{\text{BES } i}$ represent the initial and final energy in BES unit i during s, respectively.

- *Intra-stage update of the profiles of $P^t_{\text{PV } i}$ and $P^t_{\text{Load } i}$*

Each local subproblem defined by expression (2) at time step t_m employs the profile of PV generation and load for the remaining time in the stage (i.e., $\forall t \in T^s$, $t > t_m$) together with the current measurements to define the optimal operational values. An updated forecast profile is used if available. Otherwise, the available stochastic information of the decision tree is used. For this purpose, the selection of the profiles at each time step t_m is given by the Euclidean distance criterium, applied for the branches that originate from the same node of the tree (e.g., a red point in Fig. 2).

- *Warm start for the online calculation at each time step t*

A warm start scheme is adopted in the online ADMM optimization to initialize λ_i^t. Instead of using a default value of the Lagrangian multipliers for all the time steps t_m, the multipliers are initialized to the corresponding values obtained by the day-ahead multistage solution. The initial values of $\hat{P}^t_{\text{buy } i,j}$ and $\hat{P}^t_{\text{sell } j,i}$ are defined in the same way to obtain a starting value for $\overline{P}^t_{\text{exc} i,j}$.

The online optimization for each prosumer in the LEC defines the scheduling of the BES unit, the energy exchange with other prosumers and the corresponding energy exchange with the external provider, in a

coordinated way at each time step t_m.

5. Numerical tests

The presented procedures have been implemented in the AIMMS Developer environment and tested by using solver Cplex V12.9. The numerical results have been obtained on a 2.60-GHz Intel Xeon two-processors computer with 64 GB of RAM, running 64-bit Windows 10. The MIQP (mixed integer quadratic programming) solver has been employed to solve the ADMM procedures. The numerical tests included in this paper consider three different case studies: Case A, which represents a low voltage network with 2 feeders and 10 prosumers; Case B, which represents a medium voltage network with 3 feeders that connect 13 prosumers; Case C, which represents a medium voltage network with 11 feeders and 69 prosumers.

5.1. Case A: 2-feeder low-voltage network with 10 prosumers

The case study corresponds to a set of ten prosumers distributed in two feeders connected to the same substation. Configuration, prosumers, load and PV production profiles, price profile of the energy exchanges with the utility grid, and BES units characteristics are the same as in [24]. The forecasted total energy demand during the day is 313 kWh and the PV energy generation is 231 kWh (73.8% of the load). The total storage capacity installed is equal to 30 kWh. The powers are expressed in kW and the optimization horizon corresponds to one day, which is divided into 96 steps of 15 minutes each (Δt equal to 0.25 h). For the scenario-tree generation, a set of 200 scenarios has been generated for each prosumer. The scenario and decision tree is shown in Fig. 2.

The value of stochastic solution (*VSS*) and the expected value of perfect information (*EVPI*) are the typical performance metrics used to assess the effectiveness of a stochastic solution. According to e.g., [32], the *VSS* and *EVPI* are calculated as follows:

- *VSS* is the difference between *EEV* and *RP*, where *EEV* is the expected value solution and *RP* is the solution of the recourse problem (i.e., of the stochastic problem with recourse that allows corrective actions after random events have occurred). To calculate *EEV*, at first, the values of the decision variables for each t ($P_{\text{ch } i}^t$, $P_{\text{dis } i}^t$, $P_{\text{sell } i,j}^t$ and $P_{\text{buy } i,j}^t$) are obtained by the solution of the model (2) in which all input random variables ($P_{\text{PV } i}^t$ and $P_{\text{Load } i}^t$) are replaced by their expected values; then, *EEV* is the value of objective function (13) with $\ell_i^t = 0$ calculated by solving a mixed integer linear programming (MILP) problem, in which each prosumer i implements the previously calculated values of the decision variables. The imbalances at each time step t are compensated by the power exchange with the external utility grid ($P_{\text{buy\_Grid } i}^t$ and $P_{\text{sell\_Grid } i}^t$) to satisfy the power balance constraint.

14

- *EVPI* is the difference between *RP* and the wait and see (*WS*) solution given by the calculation of the expected value of the set of deterministic solutions, each relevant to one of the tree scenarios (i.e., deterministic model (2) with perfect knowledge of the PV and load profiles).

Table 2 presents the *VSS* and *EVPI* metrics calculated for case A. The resulting *VSS* shows the potential advantage of using the multistage solution over the implementation of the day-ahead forecast-based solution (i.e., *EEV*). *EVPI* indicates how close the result of the stochastic solution is to the deterministic solution assuming perfect knowledge of the PV and load profiles (i.e., *WS*).

Table 2
Stochastic metrics for Case A.

Solution	*OF* Value (€)	*VVS* (€)	*EVPI* (€)
EEV	17.07		
RP	16.55	0.52	0.09
WS	16.46		

For each scenario of the tree in Fig. 2, Fig. 4 shows the comparison between the *OF* values (i.e., daily energy procurement costs) calculated by using the day-ahead multistage solution (i.e., defining the set values at the beginning of the stage for all the time steps during the corresponding stage) and those given by the day-ahead scheduling that takes into account only the forecast profiles (forecast-based) i.e., those obtained by applying the single strategy for the entire day calculated by neglecting the uncertainties of the forecasts. As expected, the multistage scheduling provides better results with respect to a forecast-based solution. Fig. 4 also shows the *OF* values of the deterministic solution (i.e., with perfect knowledge of the PV and load profiles) of the optimization problem in equation (2).
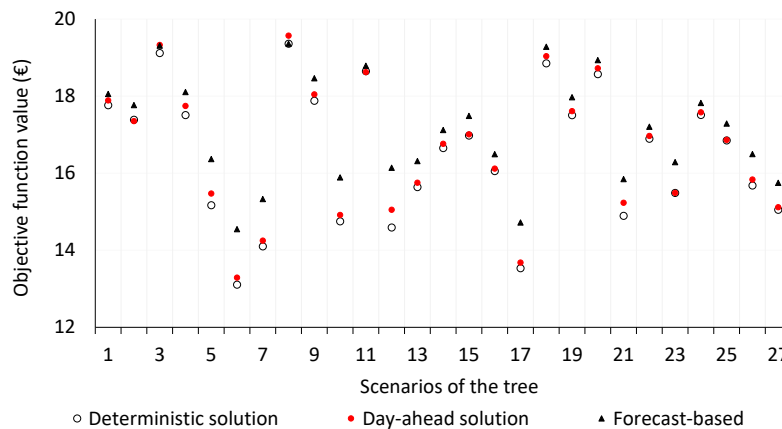

Fig. 4. Objective function value of the LEC for each scenario of the tree: Case A.

To test the operation of the intra-day decision-making approach proposed in this paper, a set with 20 new intra-day scenarios (i.e., operational conditions during the day different from those used to calculate the day-ahead decision tree) has been generated following the technique employed in Section 3. These out-of-sample

scenarios represent measurement values at each time step t for $P_{\text{PV }i}^{t}$ and $P_{\text{Load }i}^{t}$. A tolerance ε equal to 25 W has been assumed for the day-ahead calculations. A lower value of ε (10 W) is used in the intra-day optimization.

For each of these 20 new scenarios, the solutions of the intra-day procedure are compared with:

a) those obtained by using the multistage day-ahead scheduling without further online optimization;

b) those obtained by considering only the forecast profiles;

c) those obtained by considering only the forecast profiles and without allowing direct energy exchanges between the prosumers (i.e., without LEC);

d) those obtained by using a heuristic rule for charging and discharging of the batteries (i.e., without optimization) and without LEC.

Obviously, the results of all these approaches are less efficient than those obtained by assuming the perfect knowledge of the future (i.e., individual deterministic solution for each of the 20 scenarios).

For solutions a) and b), the same MILP model already described for the *EEV* calculation has been adopted, in which the decision variables are fixed, as provided by multistage day-ahead and forecast-based scheduling, respectively.

For solutions d), the implemented heuristic rule of charging and discharging actions of the individual BES units use the knowledge of the current PV generation and load as follows:

- at the beginning of the day, the BES units are assumed fully charged.

- the minimal state of charge of the BES units is set equal to 10% until 6 pm that is around three hours before the PV generation decreases to zero (according to the forecast in Case A);

- after 6 pm, the minimal state of charge of the BES units increases progressively at each time step t until it reaches 80%;

- at each time step t, each prosumer defines the values of $P_{\text{buy\_Grid }i}^{t}$, $P_{\text{sell\_Grid }i}^{t}$, $P_{\text{ch }i}^{t}$ and $P_{\text{dis }i}^{t}$ to guarantee the local power balance, with maximum use of the internal resources during t;. If PV generation is lower than demand, the charging action of the BES unit is avoided, whilst if PV generation is higher than demand the discharging action of the BES unit is avoided.

For each one of the mentioned solutions, Table 3 shows the average value of the daily energy procurement cost and the percentage increase with respect to the average value of the deterministic solutions, which is equal to € 17.23.

Table 3
OF average value in € per day obtained by employing different solutions and percentage increase with respect to the deterministic solution: Case A.

Solution	Intra-day	Multistage day-ahead (a)	Forecast-based (b)	Without LEC (c)	Without optimization (d)
OF average value (€)	17.27	17.87	17.96	21.29	31.62
Percentage increase with respect to the deterministic solution	0.23	3.71	4.25	23.51	83.52

Fig. 5 shows the comparison of the *OF* values obtained using: the deterministic model that assumes a perfect knowledge of the PV and load daily profiles, the day-ahead multistage solution (i.e., with decisions corresponding to the day-ahead tree) and the intra-day solution that includes the online rolling-horizon optimization.
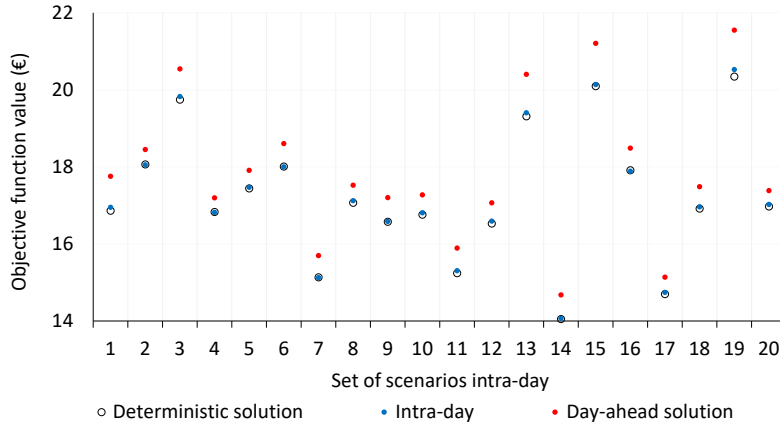

Fig. 5. Objective function value of the LEC for 20 new scenarios: Case A.

The results in Fig. 5 confirm the improved performance of the coordinated scheduling strategy with respect to the multistage solution. Additionally, Fig. 5 confirms that the coordinated strategy effectively tackles the problem associated with uncertainties in the LEC and achieves a cost-effective result very similar to the one provided by the deterministic solution with perfect knowledge of the PV and load profiles.

Since the number of variables and time horizon decrease constantly until the end of each stage (from the characteristics of the online calculation), the time employed by the online optimization at each time step t varies, on average, from around 20 seconds at the beginning of each stage to around a second at the end.

For the same 20 intra-day scenarios, Table 4 shows the average cost per day for each prosumer obtained by: the calculation without optimization, the optimization without LEC and the implementation of the intra-day solution. The implementation of the LEC, together with the intra-day approach, provides an economic

advantage for each one of the participants. The adoption of the heuristic rules and the lack of internal transactions do not allow to fully exploit the available resources.

Table 4
Average cost in € per day for each prosumer (negative value indicates revenue): Case A.

Prosumer	1	2	3	4	5	6	7	8	9	10
Without optimization	7.13	1.38	1.85	-0.13	0.16	0.06	17.14	2.54	0.08	0.40
Without LEC	5.48	0.29	1.02	-0.88	-0.46	-0.18	16.32	1.70	-0.28	-1.73
Intra-day	5.19	0.03	0.85	-1.11	-0.72	-0.26	14.63	1.60	-0.48	-2.46

5.2. Case B: 3-feeder medium-voltage network with 13 prosumers

The second test system considers the 14-bus network illustrated in Fig. 6 (adapted from [33]). The medium-voltage side of the substation has constant rated voltage equal to 23 kV. The load and PV production profiles of the prosumers, the price profiles of the energy exchanges with the utility grid and the sizes of the BES units are equal to the base case in [34]. The forecasted total energy demand during the day is 195 MWh and the PV energy generation is 56 MWh (28.7% of the load). The installed storage capacity is equal to 5.5 MWh. All the calculations refer to a time window of one day, divided into 24 steps. In this case, the tolerance ε has been defined equal to 1 kW for both the day-ahead and intra-day calculation.

Table 5 shows the resulting values of the elbow method and the silhouette coefficient (calculated for the first eight hours of the day). Three centroids have been selected to generate the scenario tree. The structure of the obtained tree is like the one of Fig. 2.
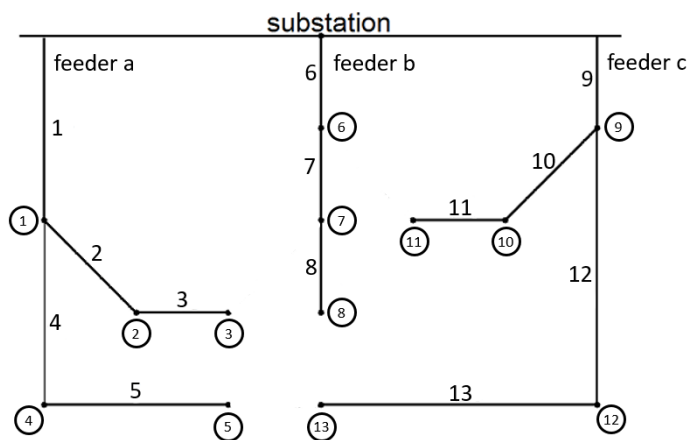

Fig. 6. Case B configuration. Circles indicate the location of the prosumers; adapted from [33].

Table 5
Elbow method and silhouette coefficient metrics for the selection of the number of clusters: Case B.

| Number of clusters	3	4	5	6	7	8	9
Average SSE	1.82	1.74	1.65	1.63	1.58	1.54	1.52
Average $s(\psi_\varphi)$	0.43	0.40	0.38	0.39	0.36	0.37	0.38

Table 6 presents the *VSS* and *EVPI* metrics calculated for case B and a tree obtained with three centroids, confirming the advantage of the stochastic solution over the forecast-based solution.

Table 6
Stochastic metrics for Case B.

Solution	*OF* Value (k€)	*VVS* (k€)	*EVPI* (k€)
EEV	45.29		
RP	45.16	0.13	0.02
WS	45.14		

Fig. 7 shows for each one of the scenarios in the tree, the comparison of the total *OF* values calculated by using the day-ahead multistage solution and those given by the forecast-based solution. As expected, the multistage scheduling provides better results with respect to the forecast-based solution. Fig. 7 also shows the corresponding *OF* value provided by the deterministic solution.
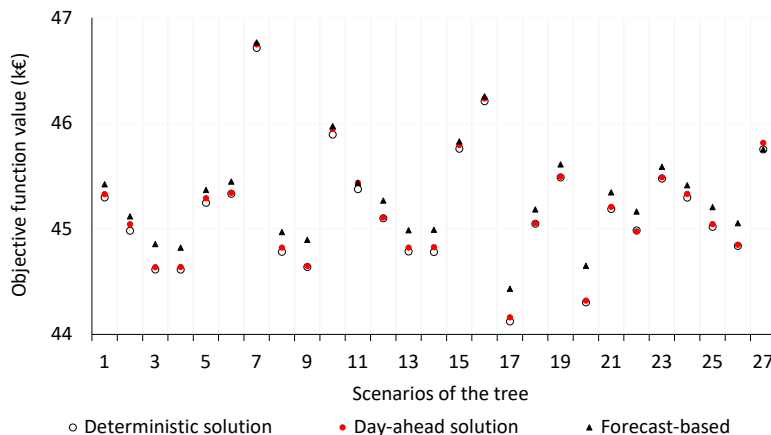
Fig. 7. Objective function value of the LEC for each scenario of the tree: Case B.

For a set of new 20 intra-day scenarios different from those used to obtain the day-ahead decision tree, Table 7 shows the average value of the *OF* value (total energy procurement cost per day) obtained by: the intra-day solution, the day-ahead multistage solution, the forecast-based solution, the optimization without energy exchanges inside the community (i.e., without LEC), and the calculation without optimization (i.e., based on basic rules for the operation of the BES units).

In the calculation without optimization, each prosumer defines its own set values following basic rules like in Case A. According to the forecast of PV generation in Case B, the minimal state of charge of the BES units is set equal to 10% until 5pm (i.e., around three hours before the PV generation decreases to zero).

Moreover, Table 7 shows, for each one of the considered solutions, the percentage increase with respect to the average value of the deterministic solution with perfect knowledge of the PV and load profiles, which is equal to k€ 44.58.

Table 7
OF average value in € per day obtained by employing different solutions and percentage increase with respect to the deterministic solution: Case B.

Solution	Intra-day	Multistage Day-ahead	Forecast-based	Without LEC	Without optimization
OF average value (k€)	44.71	44.86	44.91	48.04	52.16
Percentage increase with respect to the deterministic solution	0.29	0.62	0.73	7.76	17.00

Fig. 8 shows the comparison of the *OF* values obtained using: the deterministic model, the day-ahead multistage decision tree, and the intra-day rolling-horizon approach.
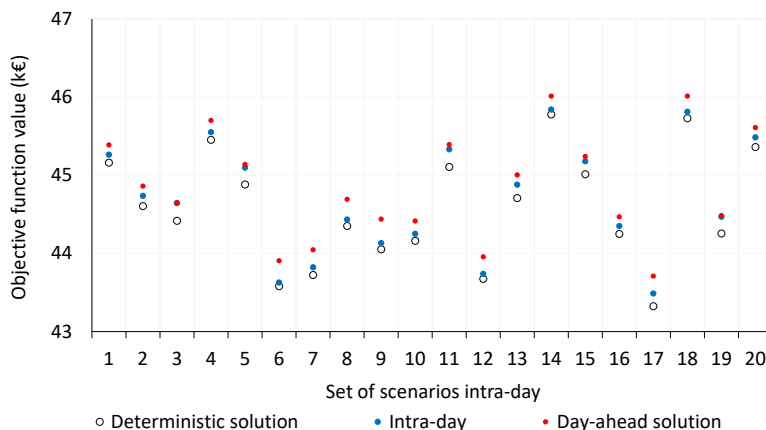

Fig. 8. Objective function value of the LEC for 20 new scenarios: Case B.

For the same set of 20 new scenarios, Fig. 8 confirms the advantage of the coordinated day-ahead and intra-day scheduling approach over the day-ahead multistage solution. The time employed by the online optimization at each time step t varies, on average, from around eight seconds to less than a second depending on the corresponding time step at which it occurs.

Table 8 shows the average daily cost for each prosumer without optimization, without internal transactions in the LEC (i.e., without LEC) and by applying the intra-day approach. The results in Table 8 show that the optimization approaches outperform the heuristic rules. Each prosumer achieves a cost reduction by participating in the LEC and implementing the intra-day approach.

Table 8

Average cost in k€ per day for each prosumer: Case B.

Prosumer	1	2	3	4	5	6	7	8	9	10	11	12	13
Without optimization	4.97	7.03	1.95	1.31	3.16	9.84	8.88	8.01	0.78	0.77	1.32	1.61	2.53
Without LEC	4.56	6.79	1.59	1.19	2.97	9.12	8.49	7.29	0.62	0.36	1.26	1.41	2.39
Intra-day	4.31	6.48	1.19	0.23	2.95	8.86	8.16	7.08	0.37	0.30	1.20	1.20	2.36

5.3. Case C: 11-feeder medium-voltage network with 69 prosumers

A third test system considers the 83-bus network shown in Fig. 9 (adapted from [35]). The medium-voltage side of the substation has constant rated voltage equal to 11.4 kV. The price profiles of the energy exchanges with the utility grid is the same as in [34], as well as the load and PV production profiles that are randomly associate to the various prosumers by adapting the corresponding maximum values to the rated ones indicated in [35]. The forecasted total energy demand during the day is 238.77 MWh and the PV energy generation is 222.22 MWh (93.06% of the load). The installed storage capacity is equal to 2.5 MWh. All the calculations refer to a time window of one day, divided into 24 steps. In this case, the tolerance ε has been defined equal to 10 kW for both the day-ahead and intra-day calculation.

Three centroids have been selected to generate the scenario tree. The structure of the obtained tree is like the one of Fig. 2 with three centroids and 27 scenarios.
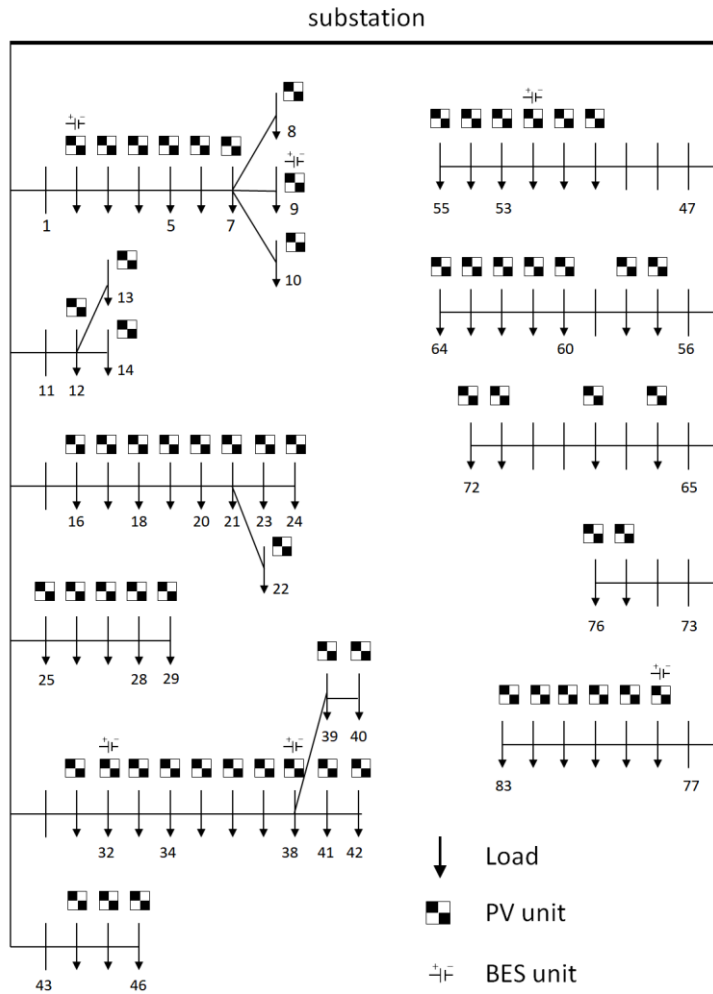
Fig. 9. Case C configuration. The sizes of the BES units (in kWh) are equal to: 300 (bus 2), 500 (bus 9), 300 (bus 32), 600 (bus 38), 500 (bus 52) 300 (bus 78).

For each scenario in the tree, Fig. 10 shows the comparison of the daily *OF* values calculated by using the day-ahead multistage solution and those given by the forecast-based solution. As expected, the multistage scheduling provides better results with respect to the forecast-based solution. Fig. 10 also shows the corresponding *OF* value provided by the deterministic solution.
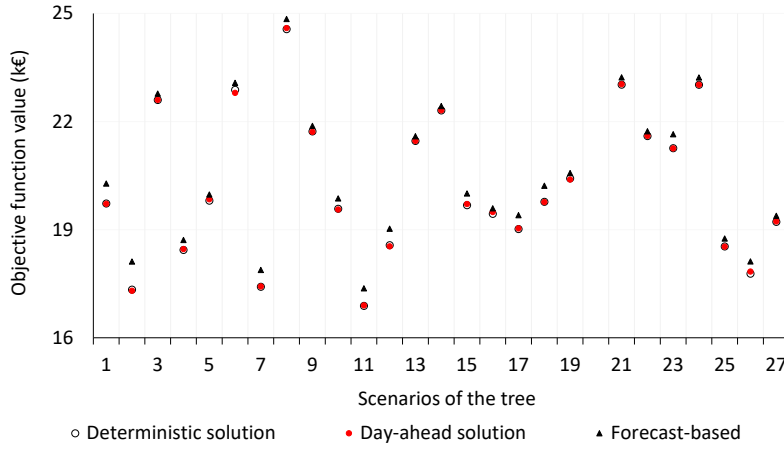
Fig. 10. Objective function value of the LEC for each scenario of the tree: Case C.

For a set of new 20 new intra-day scenarios not included in the tree, Fig. 11 confirms the advantage of the coordinated day-ahead and intra-day scheduling approach over the day-ahead multistage solution. The time employed by the online optimization at each time step t varies, on average, from around 40 second to less than a second depending on the corresponding time step at which it occurs.
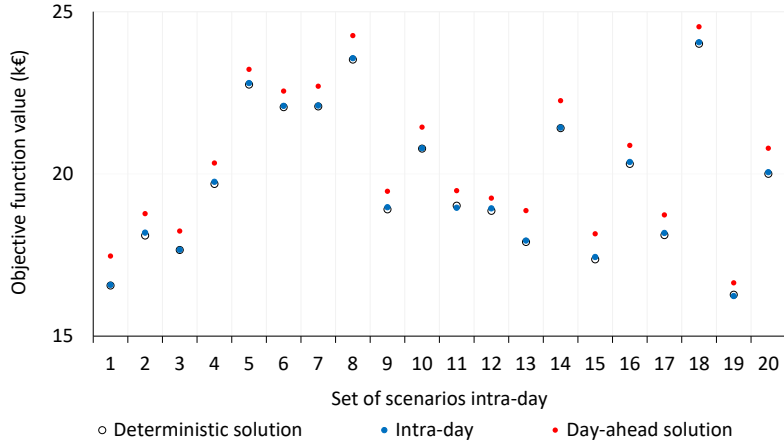

Fig. 11. Objective function value of the LEC for 20 new scenarios: Case C.

For the set of 20 new scenarios, the proposed intra-day approach gives, on average, a daily cost increment of 0.19% with respect to the deterministic solution (which is on average equal to 19.77 k€). The daily cost increment over the deterministic solution is, on average, equal to 3.20% by adopting multistage decisions based only on the day-ahead solution. Moreover, if the internal transactions in the LEC are not allowed (i.e., case without LEC), the corresponding average increment over the deterministic solution is equal to 37.80%, confirming the advantage for each participant when joining the LEC.

6. Conclusions and future work

This paper has presented a coordinated day-ahead and intra-day approach to define a cost-oriented scheduling method for a local energy community (LEC). The scheduling of the energy resources is

23

implemented by means of a distributed scheme based on the alternating direction method of multipliers (ADMM). The approach preserves the distributed and cooperative nature of the LEC throughout all the phases of the optimization, allowing each prosumer to fairly achieve an economic benefit by participating in the community.

The proposed approach has been suitably conceived to consider the uncertainties of the photovoltaic generation and energy consumption. For this purpose, a day-ahead multistage stochastic optimization (i.e., with consecutive time steps grouped according to common decisions) provides a decision tree for the next day. Subsequently, an intra-day rolling-horizon optimization defines the scheduling of battery energy storage units and exchanges of energy inside the LEC at each time step. This scheme allows to divide the optimization horizon into several stages without compromising the overall daily cost minimization. At each time step in the stage, updated information of energy generation and consumption are employed by the intra-day optimization approach.

The day-ahead multistage stochastic scheduling approach provides improved results with respect to the corresponding forecast-based solution for the LEC, which defines a single strategy for the entire day. Indeed, the multistage approach exploits the possibility take corrective decisions during the day. In the considered cases, the implemented procedure adapts the set values of the battery energy storage units and the energy transactions among the prosumers at 8 am and 4 pm, according to the current operational conditions during the day.

The intra-day procedure selects the best alternative path in the tree based on the realization of the stochastic processes (photovoltaic production and load consumption) and updated available forecasts. Indeed, in a coordinated way with the selected path among the alternative day-ahead solutions, the online intra-day procedure implements a distributed rolling-horizon optimization approach to update the scheduling at each time step. The computational time required for the intra-day optimization is short enough to be suitably implemented in a real-time energy management system.

A simple selection procedure that uses the decision tree provided by the day-ahead multistage stochastic solution can only react at the end of each stage by minimizing the cumulative difference between the profiles in the scenario tree and the current conditions during the stage. In contrast, the proposed rolling-horizon online optimization approach can also react to the fluctuations in local generation and loads at each time step.

The implementation of a specific procedure to adapt the operation of the LEC in case of operational failures, like temporary or permanent non-availability of a given resource or communication link during the day would justify a further development.

Acknowledgment

References

[1]   C. Inês, P. L. Guilherme, M. G. Esther, G. Swantje, H. Stephen, and H. Lars, "Regulatory challenges and opportunities for collective renewable energy prosumers in the EU," *Energy Policy*, vol. 138, no. December 2019, 2020.

[2]   B. Prasad, E. Koliou, J. Friege, R. A. Hakvoort, and P. M. Herder, "Energetic communities for community energy : a review of key issues and trends shaping integrated community energy systems," *Renew. Sustain. Energy Rev.*, vol. 56, pp. 722–744, 2016.

[3]   W. Tushar, T. K. Saha, C. Yuen, D. Smith, and H. V. Poor, "Peer-to-Peer Trading in Electricity Networks: An Overview," *IEEE Trans. Smart Grid*, vol. 11, no. 4, pp. 3185–3200, 2020.

[4]   F. Moret and P. Pinson, "Energy collectives: a community and fairness based approach to future electricity markets," *IEEE Trans. Power Syst.*, vol. 34, no. 5, pp. 3994–4004, 2019.

[5]   G. Belli, G. Brusco, A. Burgio, M. Motta, D. Menniti, A. Pinnarelli, and N. Sorrentino, "An energy management model for energetic communities of smart homes: the power cloud," in *Proceedings of the 2017 IEEE 14th International Conference on Networking, Sensing and Control, ICNSC 2017*, 2017, pp. 158–162.

[6]   Y. Wang, S. Wang, and L. Wu, "Distributed optimization approaches for emerging power systems operation: A review," *Electr. Power Syst. Res.*, vol. 144, pp. 127–135, 2017.

[7]   A. Kargarian, J. Mohammadi, J. Guo, S. Chakrabarti, M. Barati, G. Hug, S. Kar, and R. Baldick, "Toward distributed/decentralized DC optimal power flow implementation in future electric power systems," *IEEE Trans. Smart Grid*, vol. 9, no. 4, pp. 2574–2594, 2018.

[8]   J. Lee, J. Guo, J. K. Choi, and M. Zukerman, "Distributed energy trading in microgrids: A game-theoretic model and its equilibrium analysis," *IEEE Trans. Ind. Electron.*, vol. 62, no. 6, pp. 3524–3533, 2015.

[9]   M. Hupez, J. F. Toubeau, Z. De Greve, and F. Vallee, "A New Cooperative Framework for a Fair and Cost-Optimal Allocation of Resources within a Low Voltage Electricity Community," *IEEE Trans. Smart Grid*, pp. 1–11, 2020.

[10]   D. Vangulick, B. Cornelusse, and D. Ernst, "Blockchain for peer-to-peer energy exchanges: Design and recommendations," *20th Power Syst. Comput. Conf. PSCC 2018*, pp. 1–7, 2018.

[11]   M. L. Di Silvestre, P. Gallo, M. G. Ippolito, and E. Riva Sanseverino, "A technical approach to the energy blockchain in microgrids," *IEEE Trans. Ind. Informatics*, vol. 14, no. 11, pp. 4792–4803, 2018.

[12]   G. van Leeuwen, T. AlSkaif, M. Gibescu, and W. van Sark, "An integrated blockchain-based energy management platform with bilateral trading for microgrid communities," *Appl. Energy*, vol. 263, no. October 2019, p. 114613, 2020.

[13]   S. S. Reddy, V. Sandeep, and C.-M. Jung, "Review of stochastic optimization methods for smart grid," *Front. Energy*, vol. 11, no. 2, pp. 197–209, 2017.

[14]   A. Bhattacharya, J. P. Kharoufeh, and B. Zeng, "Managing energy storage in microgrids: A multistage stochastic programming approach," *IEEE Trans. Smart Grid*, vol. 9, no. 1, pp. 483–496, 2018.

[15]   S. Wang, H. Gangammanavar, S. D. Eksioglu, and S. J. Mason, "Stochastic optimization for energy management in power systems with multiple microgrids," *IEEE Trans. Smart Grid*, vol. 10, no. 1, pp. 1068–1079, 2019.

[16]   A. De Filippo, "Hybrid offline / online methods for optimization under uncertainty," PhD thesis - University of Bologna, 2020.

[17]   S. Fan, Q. Ai, and L. Piao, "Hierarchical energy management of microgrids including storage and demand response," *Energies*, vol. 11, no. 5, 2018.

[18]   Z. Bao, Q. Zhou, Z. Yang, Q. Yang, L. Xu, and T. Wu, "A multi time-scale and multi energy-type coordinated microgrid scheduling solution - part I: model and methodology," *IEEE Trans. Power Syst.*, vol. 30, no. 5, pp. 2257–2266, 2015.

[19]   Z. Bao, Q. Zhou, Z. Yang, Q. Yang, L. Xu, and T. Wu, "A multi time-scale and multi energy-type

coordinated microgrid scheduling solution - part II: optimization algorithm and case studies," *IEEE Trans. Power Syst.*, vol. 30, no. 5, pp. 2267–2277, 2015.

[20] W. Shi, N. Li, C. C. Chu, and R. Gadh, "Real-time energy management in microgrids," *IEEE Trans. Smart Grid*, vol. 8, no. 1, pp. 228–238, 2017.

[21] J. L. Crespo-Vazquez, T. Al Skaif, A. M. Gonzalez-Rueda, and M. Gibescu, "A community-based energy market design using decentralized decision-making under uncertainty," *IEEE Trans. Smart Grid*, pp. 1–11, 2020.

[22] A. Parisio, C. Wiezorek, T. Kyntäjä, J. Elo, K. Strunz, and K. H. Johansson, "Cooperative MPC-based energy management for networked microgrids," *IEEE Trans. Smart Grid*, vol. 8, no. 6, pp. 3066–3074, 2017.

[23] M. Khorasany, R. Razzaghi, and A. Shokri, "Two-stage mechanism design for energy trading of strategic agents in energy communities," vol. 295, no. May, 2021.

[24] S. Lilla, C. Orozco, A. Borghetti, F. Napolitano, and F. Tossani, "Day-ahead scheduling of a local energy community: an alternating direction method of multipliers approach," *IEEE Trans. Power Syst.*, vol. 35, no. 2, pp. 1132–1142, 2020.

[25] C. Orozco, A. Borghetti, F. Napolitano, and F. Tossani, "Multistage day-ahead scheduling of the distributed energy sources in a local energy community," in *2020 IEEE International Conference on Environment and Electrical Engineering and 2020 IEEE Industrial and Commercial Power Systems Europe (EEEIC / I&CPS Europe)*, 2020, vol. 675318, no. 675318, pp. 1–7.

[26] S. Boyd, N. Parikh, E. Chu, B. Peleato, and J. Eckstein, *Distributed optimization and statistical learning via the alternating direction method of multipliers*. Foundations and Trends in Machine Learning, 2011.

[27] J. M. Maciejowski, *Predictive Control: With Constraints*. Prentice Hall, 2002.

[28] C. Orozco, A. Borghetti, S. Lilla, G. Pulazza, and F. Tossani, "Comparison between multistage stochastic optimization programming and Monte Carlo simulations for the operation of local energy systems," in *2018 IEEE International Conference on Environment and Electrical Engineering*, 2018.

[29] C. Yuan and H. Yang, "Research on K-value selection method of K-means clustering algorithm," *J MDPI*, vol. 2, no. 2, pp. 226–235, 2019.

[30] B. Defourny, D. Ernst, and L. Wehenkel, "Multistage Stochastic Programming," in *Decision Theory Models for Applications in Artificial Intelligence*, IGI Global, 2012, pp. 97–143.

[31] J. L. Higle, "Stochastic programming: optimization when uncertainty matters," *Emerg. Theory, Methods, Appl.*, no. January 2021, pp. 30–53, 2005.

[32] L. F. Escudero, A. Garín, M. Merino, and G. Pérez, "The value of the stochastic solution in multistage problems," *Top*, vol. 15, no. 1, pp. 48–64, 2007.

[33] S. Cinvalar, J. J. Grainger, H. Yin, and S. S. H. Lee, "Distribution feeder reconfiguration for loss reduction," *IEEE Trans. Power Deliv.*, vol. 3, no. 3, pp. 1217–1223, 1988.

[34] M. M. Gambini, C. Orozco, A. Borghetti, and F. Tossani, "Power loss reduction in the energy resource scheduling of a local energy community," 2020, vol. 675318, no. 675318, pp. 1–6.

[35] C. T. Su, C. F. Chang, and J. P. Chiou, "Distribution network reconfiguration for loss reduction by ant colony search algorithm," *Electr. Power Syst. Res.*, vol. 75, no. 2–3, pp. 190–199, 2005.